

Liquid metal embrittlement sensitivity of the T91 steel in lead, in bismuth and in lead-bismuth eutectic

Ingrid Proriol Serre, Jean-Bernard Vogt

▶ **To cite this version:**

Ingrid Proriol Serre, Jean-Bernard Vogt. Liquid metal embrittlement sensitivity of the T91 steel in lead, in bismuth and in lead-bismuth eutectic. Journal of Nuclear Materials, 2020, 531, pp.152021. 10.1016/j.jnucmat.2020.152021 . hal-02494403

HAL Id: hal-02494403
https://hal.univ-lille.fr/hal-02494403

Submitted on 13 Oct 2020

HAL is a multi-disciplinary open access archive for the deposit and dissemination of scientific research documents, whether they are published or not. The documents may come from teaching and research institutions in France or abroad, or from public or private research centers.

L'archive ouverte pluridisciplinaire **HAL**, est destinée au dépôt et à la diffusion de documents scientifiques de niveau recherche, publiés ou non, émanant des établissements d'enseignement et de recherche français ou étrangers, des laboratoires publics ou privés.

LIQUID METAL EMBRITLLEMENT SENSITIVITY OF THE T91 STEEL IN LEAD, IN BISMUTH AND IN LEAD BISMUTH EUTECTIC

Ingrid PRORIOL SERRE, Jean-Bernard VOGT

Univ. Lille, CNRS, INRA, ENSCL, UMR 8207 - UMET - Unité Matériaux et Transformations, F-59000 Lille, France

ingrid.proriol-serre@univ-lille.fr

Corresponding author:

Ingrid PRORIOL SERRE

Univ. Lille, CNRS, INRA, ENSCL, UMR 8207 - UMET - Unité Matériaux et Transformations, F-59000 Lille, France

ingrid.proriol-serre@univ-lille.fr

Phone : +33 3 20 43 66 06

Highlights

Study of liquid metal embrittlement sensitivity of the martensitic T91 steel by Pb, Bi and LBE

The most embrittling liquid metal is LBE, then bismuth while the less one is lead

T91 steel loaded in Bi, Pb or LBE presents a ductile behaviour at 300 °C and at 400 °C except in LBE at very slow strain rate

According to the temperature and the strain rate, observation of localized brittle fracture surface in presence of LBE and Bi

Data availability

Protocols, test conditions and material characteristics are presented in detail in the text. In addition, to obtain the other research data required to reproduce the work reported in the manuscript, the readers can write to the corresponding author.

Abstract

The liquid metal embrittlement (LME) sensitivity of the martensitic T91 steel by Pb, Bi and LBE has been studied by small punch tests at different temperatures and strain rates. The LME occurrence in the three liquid metals depends on the strain rate and on the temperature. The T91 steel loaded in Bi, Pb or LBE presents ductile behaviour at 300 °C and at 400 °C except in LBE at 300 °C at very slow strain rate for which fully brittle fracture surface was observed. It appears that the LME sensitivity of the T91 steel by LBE and bismuth is more important at 300 °C than 400 °C. No LME by lead has been observed. The most embrittling liquid metal is LBE, then bismuth while the less one is lead. Some differences in the reactive wetting of the T91 steel by the saturated oxygen liquid metal could explain the difference in LME sensitivity in the three liquid metals.

Keywords

Mechanical characterization
Small Punch Test
Electron Microscopy
Fracture mode

1. Introduction

For several years, the compatibility of the T91 martensitic steel, a structural material, with liquid lead or liquid eutectic lead-bismuth (LBE) has been studied for the development of accelerated driven systems (ADS) and also some international Generational IV fission reactors (Lead-cooled Fast Reactor (LFR)) [1,2]. In this context, degradation of material properties by liquid metal is one the

issues to be clarified, especially corrosion and liquid metal-assisted fracture. Loading a ductile polycrystalline metal while immersed or after immersion in a liquid metal can give rise to the well-known liquid metal embrittlement (LME) phenomenon. The material is considered sensitive to LME when its elongation to fracture is reduced when deformed in the liquid metal instead of inert environment or when deformed in inert environment after having been in contact with the liquid metal [3-7]. Moreover, the fracture surface turns to brittle aspect in the liquid metal such as cleavage or intergranular fracture instead of ductile fracture in the inert environment. The occurrence of LME in a ductile material stressed in a liquid metal has required an intimate contact between the liquid metal and the solid metal and the application of a plastic deformation. As LME is a kind of environment-assisted fractures, it occurs for a specific set of parameters which includes the characteristics of the solid metal, those of the liquid metal and the experimental conditions. Concerning the solid metal, the most impacting parameters are the microstructure (heat treatment, grain size, cold worked or annealed), the presence or not of an oxide layer at the surface, and the roughness of the specimen. The purity and the physico-chemistry of the liquid metal influence the LME occurrence. The most influencing experimental conditions are test temperature, loading rate and loading type (uniaxial, bi-axial or tri-axial). The high number of parameters and the possible dependence between them complicate the interpretation of the LME phenomenon. For instance changing tests temperature can modify as well plasticity properties of the solid metal and at the same time viscosity of the liquid metal or oxygen content in liquid metal. Thus, a LME case pointed out for one set of experimental conditions may disappear if one of these conditions has been changed even slightly.

Legris et al. were within the first in the pointing out of LME by LBE and lead of T91 steel [8-10]. By numerical simulation at atomic scale, they estimated the effect of Pb and Bi adsorbed atoms on the surface energy of an iron surface. They concluded that LME of T91 steel by lead or LBE reflected the Rebinder effect i.e. a decrease in the surface energy of the solid alloy caused by adsorption of Pb and Bi atoms. The occurrence of LME by LBE in T91 has been reported later on by other researchers for

other sets of conditions and the fractography more deeply studied [11-23]. The brittle fracture discussed at the mesoscopic scale was either at prior austenitic grain boundaries [11,13,15,21] or transgranular. For the latter case, subtle distinctions were suggested such as cleavage [11,15,21], inter-lath fracture [20,24], quasi-brittle [20], pseudo-cleavage [25]. Occasionally, a ductile fracture with submicron dimples distinguishable from the ductile fracture in inter environment was observed [20]. From these, the range of LME mechanisms of T91 steel was enlarged and involved: reduction of the steel surface energy, and adsorption-induced reduction of the bond strength [11,13,15,21], adsorption-induced dislocation emission modification [12,19], [20,22]. Though lead and bismuth atoms exhibit close similarities, the role of each element of the liquid LBE in the occurrence of LME has been little studied. According to Legris et al calculations [10] Bi atoms should be more reactive than Pb atoms in the LME. However, the recent ToF-SIMS analysis have pointed out a preferential role of lead atoms in the LME as they were linked to oxygen dissolved in LBE [26].

Thus, in the present paper, one of the motivations is to contribute to a better understanding in the role of lead and of bismuth in the occurrence of LME of the T91 steel by LBE. The work aimed also to determine the LME sensitivity of the T91 steel in contact with Pb, Bi and LBE and to understand the difference in the influence of the 3 considered liquid metals. Small Punch Test (SPT) has been employed as mechanical test. Indeed, this test has appeared very sensitive to evidence liquid metal embrittlement [27]. Thus, some SPT were performed in the 3 liquid metals and in air. Because it has shown that the strain rate and the temperature are parameters which inhibit or increase the LME sensitivity of T91 steel by LBE [21,22], tests at different temperatures and different strain rates have been carried out.

2. Material and experiments

2.1. Material

The material we study here is the T91 martensitic steel, which is supplied in the form of rolled plates. Its chemical composition is given in Table 1. The material is considered in its standard heat treatment, performed in the laboratory : a normalizing at 1050°C for 1h followed by air cooling and a tempering for 1h at 750°C. The microstructure was revealed by Villela's reagent. It consists of tempered martensitic with a prior austenitic grain size of 15±5 µm which was determined by planimetric procedure (Figure 1). The Vickers hardness (Hv_{10}) is 278±11 Hv.

2.2. Experiments

To study the effect of the liquid metals on the mechanical properties of the steel, small punch tests (SPT) were performed. The test is based on punching a flat small specimen (10 mm×10 mm×0.5 mm) by a ball until fracture. The used SPT set up comprises a specimen holder, a pushing rod and a ball (Figure 2a). The specimen holder includes a lower die and an upper die. They are fixed by four clamping screws. The upper die with the specimen is used as the tank for the liquid metal. Contrary to the majority of SPT set-up, the load is transferred here by contact with the lower surface of the specimen. Thus, the puncher with a 2.5 mm diameter tungsten carbide ball is under the specimen. So the upper surface of the specimen in contact with the liquid metal is submitted to tensile loading. SPT were performed using an INSTRON electro mechanical machine under controlled cross-head displacement velocities of 0.0005 mm/min, 0.005 mm/min, 0.05 mm/min and 0.5 mm/min which corresponds respectively to average strain rate around of 5×10^{-6} s^{-1}, 5×10^{-5} s^{-1}, 5×10^{-4} s^{-1} and 5×10^{-3} s^{-1}.

SPT were performed in an oxygen saturated LBE (44 wt% Pb and 56 wt% Bi) bath, in oxygen saturated bismuth bath and in oxygen saturated lead bath. To avoid any contamination which could affect the results, a specific SPT specimen holder was dedicated to each liquid metal. Furthermore, between each test, the SPT specimen holder was cleaned. To obtain an homogeneous temperature of the SPT set-up (lower die, upper die, specimen, ball, and environment) and so for small punch tests at

high temperature, a heat ring was used. To perform tests at different temperatures: 250 °C, 300 °C and 400 °C, the temperature was controlled by a thermocouple placed in the environment (the liquid metal or air), and 3 mm away from the upper surface of the specimen.

The LME occurrence depends on the surface state of the solid alloy. Thus, in order to avoid effects due to the roughness of the surface and residual stresses developed during the mechanical polishing, SPT specimens were mechanically polished with SiC paper up to 1200 grade, and then polished step by step with suspension diamond pastes liquid to 1 µm. The final thickness of the specimen before testing was around 500±10 µm. The procedure for heating the SPT specimen consisted in the heating up the specimen and the SPT set-up from room temperature to the targeted test temperature at a heating rate, between 7 °C/min and 9 °C/min and in holding then for 10 minutes before SPT. After test, the cooling down to room temperature was performed without temperature control. Load – cross-head displacement curves were recorded during tests.

After test, the fracture surfaces were analysed by scanning electron microscope (SEM). Prior to the SEM examinations, to remove the solidified LBE, bismuth or lead present on the fracture surface and on the surface of the sample, the SPT specimens tested in liquid metal were cleaned in a solution containing CH_3COOH, H_2O_2 and C_2H_5OH at a ratio of 1:1:1.

Given the literature data, the reference conditions were: air or LBE at 300 ° C and 400 ° C, and for 0.5 mm / min. For these conditions at least three tests were carried out. For the other conditions, the tests were at least duplicated when a phenomenon or evolution suggesting an effect of the liquid metal was observed. The curves shown in the following figures are the curve of a test representative of all the SPT curves obtained with the same conditions. The values in Tables 2, 3 and 4 represent the average of the values of all the tests performed for the condition if several tests and otherwise the value of the single test.

3. Results

3.1. Tests at 300 °C

Figure 3 presents the load – cross-head displacement curves recorded during the SPT tests in liquid bismuth and in liquid LBE at 300°C for the four different displacement speeds.

In bismuth, the SPT curves (Figure 3a) exhibited for the four displacement speeds a ductile behavior [27-30] with the presence of the 4 typical stages of the SPT curve of ductile materials noted "❶", "❷", "❸", "❹" on the schematic curve (Figure 2b). The stages correspond to : 1. the elastic bending, 2. the plastic bending, 3. the stretching of the membrane, 4 the formation and propagation of the main crack. Note that microcracks initiation for ductile metallic materials occurs during the stage 3 [31].

To evaluate the influence of the strain rate, the typical values measured from the curves (Figure 2b) such the maximum load F_{max}, the displacement at the maximum load d_f and the energy at the maximum load J_{fmax} (area under the load versus displacement curve until F_{max}) were determined (Table 2). The maximum load F_{max}, the displacement at the maximum load d_f and the energy at the maximum load J_{fmax} decreased with the decreasing of the strain rate. Then, the mechanical resistance and the ductility were more important for the higher displacement speeds i.e. the higher strain rates. It was possible to link this evolution with the fracture mode of the specimens (Figure 4). At 0.5 mm/min, the main crack was circular accompanied with a very small radial cracks (Figure 4a); the fracture was ductile with the presence of dimples (Figure 4b). At 0.05, 0.005 and 0.0005 mm/min, some radial cracks decorated the main circular crack (Figures 4e and 4c). The fracture was ductile but some brittle fracture surfaces were observed near the surface of the sample in contact with the liquid bismuth (Figures 4d and 4f).

For the tests in liquid LBE, the SPT curves (Figure 3b) showed a strong dependence on displacement speed. For the 3 highest strain rates, the SPT curves exhibited a ductile behaviour. But, the curve of the test performed at the lowest speed (0.0005 mm/s) was clearly distinguishable from the three other

ones. First, the maximum load was strongly reduced as compared to the other tests performed at higher speeds by a factor of two-third. Secondly, the displacement at the maximum load was decreased in the same way. Thirdly, the curve exhibited a pop-in during the beginning of the stage 2. These results were confirmed by repeating three times the test. As well, the typical values of the test performed at the lowest speed were strongly smaller than those for the three higher speed tests. For the three latter, no significant variation was observed between them (Table 2). This suggests a falling of the mechanical resistance and of the ductility when the displacement reaches 0.0005 mm/min. All the SPT specimens fractured in LBE exhibited circular and radial cracks. The decrease in the strain rate promoted radial cracking (Figure 5). So, the number of radial cracks for the test performed at 0.0005 mm/min was much reduced as compared to the other tests and the radial cracks were also much longer (Figure 5g). In addition, the fracture surface presented fully brittle aspect (Figure 5h). For the higher displacement speeds, the fracture surface was ductile but some brittle fracture zones were observed but only near the surface of the specimen in contact with the liquid LBE.

3.2. Tests at 400 °C

The macroscopic behavior of the T91 steel in the liquid bismuth reflects a ductile response (Figure 6a). The curves exhibit the same shape and the typical values of the SPT are of the same order (Figure 6c and Table 3). But, the maximum load F_{max}, the displacement at the maximum load d_f and the fracture energy at the maximum load J_{fmax} were less important at 0.005 mm/min and more important at 0.0005 mm/min (Table 3). It was impossible to make a link between these observations and the modes of fracture. Indeed, in all conditions, the main crack was circular (Figure 7a, Figure 7c, Figure 7i, Figure 7j), the fracture surface ductile (Figure 7b). Some radial cracks were observed for the specimens tested at 0.0005, 0.005 and 0.5 mm/min (Figure 7c, Figure 7i, Figure 7j). The radial cracks were longer at 0.005 mm/min, and very small at 0.0005 mm/min (Figure 7i, Figure 7j). Very local brittle fracture zones were observed at 0.5 mm/min (Figure 7d).

In LBE, for all studied displacement speeds, the SPT curves (Figure 6b) exhibit a ductile behaviour. No pop-in was observed. The displacement velocity did not affect the mechanical behavior even though some of the typical values measured from the curves (F_{max}, d_f and J_{fmax}) have varied a little bit (Table 3). The main crack was circular with some radial cracks observed at the three higher displacement speeds (Figure 7e, Figure 7k). The facture surface was ductile. Some very localized brittle fracture surfaces has been observed near the surface in contact with the liquid metal at 0.5 and 0.05 mm/min (Figure 7f).

The macroscopic behaviour of the T91 steel in liquid lead at 400 °C suggests a ductile behaviour (Figure 6c) confirmed by the fracture mode where dimples and a main circular crack can be seen (Figure 7g, Figure 7h, Figure 7l). Only the SPT specimen tested at a speed of 0.005 mm/min contained a circular crack decorated by very small radial crack. No fracture surface with a brittle aspect has been observed in presence of liquid lead. The characteristic values of the curves vary very little according to strain rate except for 0.0005 mm/min (Table 3). This is coherent with the observations of the surface fractures.

For tests at 400 °C in bismuth and in lead, the SPT characteristic values were larger at 0.0005 mm / min, without the fracture surface being able to explain this shift in the values (Table 3). This effect is also observed in presence of LBE, but less drastically. At 300 °C, the highest values are obtained for tests in bismuth and LBE performed at the highest speed (0.5 mm/min) (Table 2). For each liquid metal considered separately at a given strain rate, except these two peculiar situations, the mechanical properties of the T91 steel do not vary so much. The tests performed at 400 °C and at a speed of 0.0005 mm/min lasted about 50 hours, which resulted in an important oxidation of the liquid metal especially for the lead. This presence of a large contain of oxides could be explained by an increase of the load (F_{max}) for the tests at the lowest strain rate.

3.3. Tests at 250 °C

Complementary Small Punch tests at 250 °C in LBE were carried out in the same range of displacement speeds for the T91 steel (Table 4, figures 8 and 9). For all the studied cases, the curves reflect a ductile behavior. Differences in the characteristic values were minor except for the test carried out at the displacement speed of 0.5 mm/min where d_f and f_{max} were much higher. In addition, radial cracks were absent for this test while they formed for the other ones and their length increased with the decrease in displacement speed. The fracture surface was ductile. Except the specimen fractured at 0.5 mm/min, local brittle fracture surfaces near the surface initially in contact with the liquid metal was observed.

4. Discussion

The present investigation employed the small punch test technique and fractographic analysis to investigate the sensitivity of T91 steel to LME by Pb, Bi and LBE at 300 °C and 400 °C and for a displacement speed range between 0.5 mm/min and 0.0005 mm/min. At first glance, the mechanical response suggests a ductile behaviour of the material except when loaded in LBE at 0.0005 mm/min. However, paying close attention to the variations in mechanical values, to crack pattern at the specimen dome and to the fracture surface allow pointing out a certain degree of sensitivity to embrittlement according to the considered liquid. And for a considered liquid metal, it depends on the test conditions, strain rate, temperature.

To evaluate the sensitivity of LME according to the liquid metal (lead, LBE or bismuth), we determined according to the SPT load/displacement curves the normalized energy at the maximum force (fracture energy per thickness unit) $J_{fmaxNorm}$. This value represents the energy (per thickness) for the elastic deformation and plastic deformation of the sample and for the initiation of the micro-cracks and cracks which can lead to macroscopic damage of the sample. Figures 10 and 11 show respectively at 300°C and 400°C the evolution of the normalized fracture energy $J_{fmaxNorm}$ according to the

displacement speed, and according to the environment. A representation of the fracture mode is present for all cases. The values of $J_{fmaxNorm}$ for the different conditions are reported in Table 2 and in Table 3 in which previous results of SPT performed in air and at 0.5 mm/min have been included. From the literature [13,14,32], the monotonic mechanical properties in air at 400°C and at 300°C do not change so much with the studied strain rates. Thus, one can consider the values obtained during SPT in air and at 0.5 mm/min. representative of the data in air at the other three studied strain rates.

For all conditions of temperature and strain rate, the presence of liquid metal (Pb or Bi or LBE) impact the characteristic values of the SPT curves of T91 steel. All the values of F_{max}, d_f and $J_{fmaxNorm}$ decrease when the tests were performed in a liquid metal instead of air as it has been reported in the past by Ye et al [21] for LBE. Fracture modes in T91 steel tested in LBE at 300°C exhibited the fully brittle fracture surface at a displacement velocity of 0.0005 mm/min to mostly ductile fracture for the other displacement velocities. At 300 °C in liquid bismuth, the fracture is fully ductile for the test performed at 0.5 mm/min but contains some brittle zones localized near the surface in contact with the metal liquid for the other displacement speeds. At 400 °C, no fully brittle fracture surface has been observed. The facture surfaces are generally ductile except in liquid bismuth at 0.5 mm/min and in liquid LBE at 0.5 and 0.05 mm/min for which some brittle zones were observed. For the martensitic T91 steel, LBE appears to be the most embrittling liquid metal at 300 °C and at 400 °C.

The test temperature has a great importance in the appearance or not of the LME [4,7]. In fact, the ductility of the solid metal in air, the wetting of the solid alloy by the liquid metal, and the liquid metal / solid metal chemical interactions which influence the LME occurrence, depend on the temperature. An increase in temperature generally favors the ductility of materials. Indeed, a crack propagates more difficult in a ductile material because of plastic deformation at the crack tip which blunts. Thus, generally, LME is manifested by a trough of ductility more or less wide in temperature,

the starting temperature of which is the melting temperature of the liquid metal. LME gradually disappears at temperatures for which the dislocation activity is sufficient to promote plastic deformation and so ductile failure. Furthermore, it is known that sensitivity to LME is often maximum close to the melting point of the liquid metal [4]. In the present study, the most embrittling liquid metal seems to be LBE and the least one lead. However, the three investigated liquid metals have different melting temperatures (Pb: 327 °C, Bi: 271 °C, LBE: 125 °C). We can not exclude that our conclusion is distorted by the relationship between the considered test temperatures and the melting temperature of each liquid metal. This is why we evaluated the position of the test temperatures in respect to the ductility tough, for each of the three liquid metals.

In the case of the T91 steel studied in contact with LBE, the intensity and the temperature for which the effect of LBE is the most important vary according the authors and so the experimental conditions (strain rate, type of loading, sample geometry, oxygen concentration in LBE, roughness state …) [13,17,18,33,34]. According to the different results, the temperature range for which the LME sensitivity of the T91 steel by LBE is the most important is between 300 °C and 350 °C. From this study, it appears that LME sensitivity of the T91 steel by LBE is more important at 300 °C (figures 3b and 5) than at 250°C (Figures 8 and 9). These results are in agreement with other researches where it was observed that LME of T91 steel is more pronounced between 300 °C and 350 °C.

No data has been found on the behavior of the T91 steel in the presence of liquid bismuth. Some cases of LME by bismuth for other steels have been only reported by Old [5]. Furthermore the LME sensitivity by the liquid bismuth of the Armco iron has been studied by Popovich et al. who have shown a large effect of the temperature on LME occurrence [35,36]. In the present study, the effect of bismuth is more important at 300 °C than at 400 °C. Furthermore, the melting temperature of bismuth is 271 °C, a temperature close to the test temperature 300 °C. So we can assume that the studied temperature range corresponds to the ductility trough of the T91 steel in the presence of liquid bismuth.

In some researches [9,37-39], the susceptibility of T91 steel to LME in liquid Pb has been studied. Vogt et al. studied the behavior between 350 °C and 550 °C in oxygen saturated lead of the T91 steel hardened by a tempering at 500 °C by using notched tensile specimen. Hojna et al. investigated the LME sensitivity of the T91 steel (in its standard heat treatment annealed at 770°C) after surface pre-treatment to obtain Pb wetting, in lead with a low content of oxygen (from 10^{-11} to 10^{-7} wt. %) by applying slow loading rate, with smooth and notched specimens. With notched specimens, LME has been observed between 350 °C and 400 °C by Hojna and Di Gabriele. The severity of LME was expected to be greater at 350 °C than at 400 °C [37,38]. Vogt observed that the return to ductility is progressively effective starting from 425 °C (mixed ductile brittle fracture surface) and the steel is ductile in the lead at 450 °C [9]. Note that the conditions of the tests in the present study are different from the studies previously cited in terms of microstructure of material, surface conditions, presence of notch, content of oxygen in lead. In particular, the most important differences having a significant effect on LME occurrence are 1. the initial surface state of the T91 steel, in terms of wetting effect [16], 2, strain rate [21], 3. presence or not of a notch and therefore tri-axial stress [8]. So the comparison between the different results is not easy. In the present study, the experimental conditions of tests are close to those of Vogt in terms of strain rate and oxygen content in lead, and the microstructure of the steel from that of Hojna and Di Gabriele. But SPT specimens are not notched. So, according to the different results, we can assume that the test temperature of 400 °C of the present study is in the ductility tough but is not necessarily the detrimental one for LME.

The test temperature 300°C is in the ductility trough of the T91 steel in contact with LBE and Bi and is the most detrimental in terms of LME. At 300°C, we can conclude unambiguously that LBE is more embrittling than the liquid bismuth. For the test temperature of 400 °C and for each liquid metal, T91 steel is in the ductility tough but we observe a return to ductility. Clearly, at 400°C, LBE is the most embrittling liquid metal. Because of the surface observations and because 400 °C is a temperature

much closer to the melting temperature of lead than bismuth, we can conclude that bismuth is more embrittling than lead for the T91 steel.

The most embrittling liquid metal is LBE while the less one is lead. The present conclusion based on experimental evidence differs from that given by Legris et al [10] who employed ab initio atomic scale simulations combined to a thermodynamic model and turned the T91 steel to pure iron. Indeed, they found that bismuth had the most important impact on LME of iron, then LBE and finally lead [10]. In their study, the embrittling criterion was built on a LME model based on the reduction of the surface energy by liquid metals adsorption. They also ignored the presence of oxygen which has an influence on the sensitivity of the T91 steel by the LBE [21-23].

To understand the difference in LME sensitivity of the T91 steel between Pb, Bi and LBE, we compared the properties of the three liquid metals and their interactions with the steel.

The chemical and physical properties of Pb, Bi and LBE, collected in Chapters 2 and 3 of the Handbook [40,41], are very close. Indeed, it is found that the affinity of Pb and Bi for Fe and Cr are similar [41,42]. The calculated chemical activity (which expresses the difference between the properties of the pure element or in a mixture compared to a standard state) of Pb and Bi in LBE reported in Table 5 are not very influenced by the temperature. The values are slightly larger for bismuth than for lead. This result could suggest a behavior of LBE closer to that of Bi than that of Pb.

The sensitivity to LME depends on the wettability of the solid material by the liquid metal [3,6,7]. Among the different factors that affect the wettability, surface tension plays an important role. Then, the higher the surface tension of the liquid metal, the less the liquid metal has the ability to wet surfaces. From the data given in [40], the surface tensions of Bi, Pb and LBE at 250 °C, 300 °C and 400 °C have been calculated (Table 6). The metal with the highest surface tension is Pb, which could explain the quasi-absence of LME of T91 steel in contact by lead by comparison with Bi and LBE. However, at 300 °C, bismuth has a lower surface tension than LBE whereas LBE is more embrittling.

In addition, the value of the surface tension of bismuth at 400 °C is lower than that of LBE at 300 °C while a very low sensitivity of the T91 steel by Bi was observed at 400 °C. Thus, the value of the surface tension, an element to explain the wettability by the liquid metals, cannot explain the differences in sensitivity of the studied steel in the three studied liquid metals. Furthermore, generally, similar values of wetting measured on iron surfaces for liquid Pb, LBE and Bi are reported in the literature [43-45]. This is due to the resemblance of interactions of Pb and Bi with iron. Neither Pb nor Bi form intermetallics with iron, and the solubility of iron in liquid Pb-Bi is very close to the solubilities in liquid Pb and liquid Bi. No reactive wetting occurs.

The influence of oxygen content in LBE on the corrosion resistance and on the LME sensitivity of the T91 steel has been studied [21-23,46]. A low oxygen content in LBE increases the sensitivity to corrosion and LME of T91 steel in LBE. Indeed, low oxygen content limits the re-formation of oxide destroyed by plastic deformation and then improves contact between the steel and the liquid metal. In the present study, the liquid metals were in contact with air and so saturated in oxygen. We calculated the oxygen solubility limit in molten lead, bismuth and LBE according to the recommended formula in [41] (Table 7). The main points are that for the three liquid metals, at 250 °C, 300 °C and 400 °C, the oxygen contents at saturation are close and are sufficient to allow oxide formation at the fresh surfaces of the steel deformed in liquid metal and so to avoid intimate contact between the steel and the liquid metal. Furthermore Martinelli et al. [47] showed that the oxygen solubility in LBE depended on the lead content. They found that the composition of Pb-Bi alloys did not affect the composition and the mechanisms of oxide formation at the steel surface oxide but only the oxidation rate. Thus, the differences in results obtained with the three liquid metals cannot be linked to a re-oxidation difficulty of the fresh surfaces of the T91 steel deformed in liquid metal. However, despite some dispersions in the data, it seems to show that the diffusion coefficient of oxygen is greater in LBE than in Bi and Pb [41]. This could suggest that oxidation of fresh surfaces is easier in LBE and therefore a lower LME sensitivity in this environment, which was not observed in our study. It has

been shown that pure Pb without oxygen do not wet the T91 steel surface because of the presence of $FeCr_2O_4$ oxide film onto the T91 steel surface but wet the surface of iron free of all oxide layer [48]. However it has been shown that Pb, Bi and LBE containing dissolved oxygen can wet oxides present on the surface of steels (iron oxide and chromium-iron oxide) [44,49]. Indeed, contrary to what is observed for metallic surfaces without oxide, steels covered by an oxide layer could be better wetted by a liquid metal (Pb, Bi and LBE) containing dissolved oxygen because of the attraction between oxygen in liquid metal and oxygen in oxide giving rise to a reactive wetting. Thus, the dissolved oxygen in liquid metal can influence LME process either by limiting the metallic surface re-oxydation (very low oxygen), or by promoting reactive wetting between liquid metal containing dissolved oxygen and oxide surface of the steel. The present study fits with the last situation because ours tests were performed in liquid metal saturated in oxygen.

Some studies report the difference in the role of Pb and Bi on LME by LBE or on corrosion by LBE. From corrosion experiments on the T91 steel immersed in LBE at 470°C during 3700 hours, SIMS analyses showed the presence of lead but not bismuth inside the oxide layer. In other words, the oxide layer acted as a “filter” retaining lead and allowing passage of bismuth [50]. Note that lead was retained only in the oxides formed in oxygen saturated Pb–Bi alloy while bismuth was found in the oxides formed by oxidation in oxygen saturated liquid bismuth. ToF-SIMS analyses showed the penetration of lead and/or bismuth beneath the surface of the T91 steel immersed in LBE (with low oxygen content: 10^{-8} w%) [26]. The authors concluded to a most likely lead adsorption at the surface of the oxide layer than bismuth adsorption. Furthermore oxygen in low quantity could drive the lead atoms to the surface and then to the bulk of the steel. These two studies [26,50] show clearly a preponderant effect of lead linked to the presence of oxygen in the liquid metal. Note that PbO exhibits a higher stability than Bi_2O_3. Furthermore molecular oxygen (O_2) dissolves in LBE in the form of a monoatomic species (O) with electronegativity significantly higher than that of lead and bismuth. Therefore, the electrons of the outermost electronic shell of Pb atoms will be attracted by O

atoms and oxygen will be present in the liquid metal in the form of O_2- ions. In the liquid LBE, oxygen is preferentially linked to Pb atoms rather than to Bi atoms. Thus, in LBE, Pb-O couple can be preferentially attracted at the oxide layer present at the surface of the T91 steel for adsorption than Bi. The Pb is absorbed in the layer and then in the steel which allows LME occurrence [26].

In the present study, the liquid metals were saturated in oxygen. The difference of LME sensitivity by lead and LBE could be explained by the presence of more dissolved oxygen link to the Pb in LBE and so more attraction of the Pb-O couple by the oxide at the surface of the T91 steel. Furthermore, the results are coherent with results reported by Old [5] concerning the LME sensitivity of the AISI 4140 steel at 370°C. Therefore for the AISI 4140 steel, LME sensitivity is increased by additions of bismuth to lead. Concerning the liquid bismuth, a small number of studies have been carried out on the behavior of the T91 steel in contact with bismuth (corrosion) and on the wettability of this steel by liquid bismuth. In addition, the test temperatures differed from our tests. The observations presented in our study tend to show a greater reactive wetting of the oxided surface of the steel by lead than by bismuth. However, this result cannot be verified experimentally or cannot be correlated by the results of the literature. The more important reactive wetting of the oxided surface of the T91 steel by lead could explain that the more embrittling liquid metal is LBE and then bismuth.

5. Conclusions

The LME sensitivity of the T91 steel by Pb, Bi and LBE has been studied with the SPT technique and the observations of the fractured specimens. The effects of strain rate (by changing the displacement speed from 0.5 mm/min to 0.0005 mm/min) and of test temperature (250°C, 300°C, 400°C) on the sensitivity of LME have been considered.

The main conclusions are:

- All SPT curves exhibit nearly the same shape which did not allow suspecting LME.

- The normalized fracture energy calculated from the SPT curve depends on the test conditions but is not satisfactory enough to predict LME occurrence.
- Three morphologies of fracture surface are observed: fully ductile, fully brittle and small area of brittle fracture surface in a ductile fracture surface.
- A pronounced LME with a fully brittle fracture surface is found with LBE at 300°C and a displacement speed of 0.0005 mm/min.
- T91 steel is more sensitive to LME by LBE and bismuth at 300 °C than 400 °C.
- The most embrittling liquid metal is LBE, then bismuth while lead is the less one.
- Some differences in the reactive wetting of the T91 steel by the saturated oxygen liquid metal may be the source in the difference in LME sensitivity between the three different liquid metals.

Acknowledgment

For their participation to this study, the authors thank Dr C. Ye, Ing. J. Golek and D. Creton.

Funding

A financial support to this study has been brought by the french National Center for Scientific Research, the Lille University (France) and the National Graduate School of Engineering Chemistry of Lille (France).

Data availability

The data required to reproduce this work can be requested from the corresponding author.

Declaration of competing interest

The authors declare that they have no known competing/financial interests or personal relationships that could have/appeared to influence the work reported in this paper.

References

[1] F.J. Martín-Muñoz, Chapter 6: Compatibility of structural materials with lead-bismuth eutectic and lead: Standardisation of data, corrosion mechanism and rate, in Handbook on lead–bismuth eutectic alloy and lead properties, materials compatibility, thermal-hydraulics and technologies, OECD/NEA, 2015, pp. 431-486.

[2] J-B. Vogt, I. Proriol Serre, D. Gorse, Chapter 7: Effect of lead-bismuth eutectic and lead on mechanical properties of martensitic and austenitic steels, in Handbook on lead–bismuth eutectic alloy and lead properties, materials compatibility, thermal-hydraulics and technologies, OECD/NEA, 2015, pp. 487-570.

[3] M.H. Kamdar, Embrittlement by liquid metals, Prog. Mater. Sci. 15(4) (1973) 289-374.

[4] M. Nicholas, C. Old, Liquid metal embrittlement, J. Mater. Sci. 14(1) (1979) 1-18.

[5] C.F. Old, Liquid metal embrittlement of nuclear materials, J. Nucl. Mater. 92(1) (1980) 2-25.

[6] P.J.L. Fernandes, R.E. Clegg, D.R.H. Jones, Failure by Liquid Metal Induced Embrittlement, Eng. Fail. Anal. 1-1 (1994) 51-63.

[7] B. Joseph, M. Picat, F. Barbier, Liquid metal embrittlement: A state of the art appraisal, Eur. Phys. J. 5 (1999) 19-31.

[8] G. Nicaise, A. Legris, J-B. Vogt, F. Foct, Embrittlement of the martensitic steel 91 tested in liquid lead, J. Nucl. Mater. 296 (2001) 256-264.

[9] J-B. Vogt, G. Nicaise, A. Legris, F. Foct, The risk of liquid metal embrittlement of the Z10CDNbV 9-1 martensitic steel, J. Phys IV 12 (2002) 217-225.

[10] A. Legris, G. Nicaise, J-B. Vogt, J. Foct, Liquid metal embrittlement of the martensitic steel 91: influence of the chemical composition of the liquid metal. Experiments and electronic structure calculations, J. Nucl. Mater. 301(1) (2002) 70-76.

[11] T. Auger, G. Lorang, Liquid metal embrittlement susceptibility of T91 steel by lead–bismuth, Scripta Mater. 52(12) (2005) 1323-1328.

[12] A. Verleene, J.-B. Vogt, I. Serre, A. Legris, Low cycle fatigue behaviour of T91 martensitic steel at 300°C in air and liquid lead bismuth eutectic, Int. J. Fatigue 28 (2006), 843-851.

[13] Y. Dai, B. Long, F. Gröeschel, Slow strain rate tensile tests on T91 in static lead-bismuth eutectic, J. Nucl. Mater. 356 (2006) 222-228.

[14] J. Van den Bosch, D. Sapundjiev, A. Almazouzi, Effects of temperature and strain rate on the mechanical properties of T91 material tested in liquid lead bismuth eutectic, J. Nucl. Mater. 356 (2006), 237-246.

[15] I. Serre, J.-B. Vogt, Heat Treatment Effect of T91 martensitic steel on Liquid Metal Embrittlement, J. Nucl. Mater. 376 (2008) 330-335.

[16] T. Auger, I. Serre, G. Lorang, Z. Hamouche, D. Gorse, J.-B. Vogt, Role of oxidation on LME of T91 steel studied by Small Punch Test, J. Nucl. Mater. 376 (2008) 336-340.

[17] B. Long, Z. Tong, F. Gröschel, Y. Dai, Liquid Pb-Bi embrittlement effects on the T91 steel after different heat treatments, J. Nucl. Mater. 377 (2008) 219-224.

[18] D. Gorse, T. Auger, J-B. Vogt, I. Serre, A. Weisenburger, A. Gessi, P. Agostini, C. Fazio, A. Hojna, F. Di Gabriele, J. Van Den Bosch, G. Coen, A. Almazouzi, M. Serrano, Influence of liquid lead and lead–bismuth eutectic on tensile, fatigue and creep properties of ferritic/martensitic and austenitic steels for transmutation systems, J. Nucl. Mater. 415(3) (2011) 284-292.

[19] A. Hojna, F. Di Gabriele, On the kinetics of LME for the ferritic–martensitic steel T91 immersed in liquid PbBi eutectic, J. Nucl. Mater. (2011) 21-29.

[20] X. Gong, P. Marmy, A. Volodin, B. Amin-Ahmadi, L. Qin, D. Schryvers, S. Gavrilov, E. Stergar, B. Verlinden, M. Wevers, M. Seefeldt, Multiscale investigation of quasi-brittle fracture characteristics in a 9Cr–1Mo ferritic–martensitic steel embrittled by lead–bismuth eutectic under low cycle fatigue, Corros. Sci. 102 (2016) 137-152.

[21] C. Ye, J-B. Vogt, I. Proriol Serre, Liquid metal embrittlement of the T91 steel in lead bismuth eutectic: The role of loading rate and of the oxygen content in the liquid metal, Mat. Sci. Eng. A 608 (2014) 242-248.

[22] X. Gong, P. Marmy, B. Verlinden, M. Wevers, M. Seefeldt, Low cycle fatigue behavior of a modified 9Cr–1Mo ferritic–martensitic steel in lead–bismuth eutectic at 350 °C – Effects of oxygen concentration in the liquid metal and strain rate, Corros. Sci. 94 (2015) 337-391.

[23] J-B. Vogt, J. Bouquerel, C. Carlé, I. Proriol Serre, Stability of fatigue cracks at 350 °C in air and in liquid metal in T91 martensitic steel, Int. J. Fatigue (2020) 105265

[24] M.L. Martin, T. Auger, D.D. Johnson, I.M. Robertson, Liquid-metal-induced fracture mode of martensitic T91 steels, J. Nucl. Mater. 426(1-3) (2012) 71-77.

[25] Z. Hadjem-Hamouche, T. Auger, I. Guillot, Temperature effect in the maximum propagation rate of a liquid metal filled crack: The T91 martensitic steel/Lead–Bismuth Eutectic system, Corros. Sci. 51(11) (2009) 2580-2587.

[26] I. Proriol Serre, J.-B Vogt, N. Nuns, ToF-SIMS investigation of absorption of lead and bismuth in T91 steel deformed in liquid lead bismuth eutectic, Appl. Surf. Sci. 471 (2019) 36-42.

[27] I. Serre, J-B. Vogt, Liquid Metal Embrittlement of the T91 martensitic steel evidenced by the Small Punch Test, Nucl. Eng. Des. 237 (2007) 677-685.

[28] T. Misawa, T. Adachi, M. Saito, Y. Hamaguchi, Small punch tests for evaluating ductile-brittle transition behavior of irradiated ferritic steels, J. Nucl. Mater. 150 (1987) 194-202.

[29] G.E. Lucas, Review of small specimen test techniques for irradiation testing, Metall. Trans. A 21A (1990) 1105-1119.

[30] X. Mao, J. Kameda, Small-punch technique for measurement of material degradation of irradiated ferritic alloys, J. Mater. Sci. 26 (1991) 2436-2440.

[31] I. Penuelas, I.I. Cuesta, C. Betegon, C. Rodriguez, F.J. Belzunce, Inverse determination of the elastoplastic and damage parameters on small punch tests, Fatigue Fract Engng Mater Struct 32 (2009) 872-885.

[32] O. Hamdane, J. Bouquerel, I. Proriol Serre, J-B. Vogt, Effect of heat treatment on liquid sodium embrittlement of T91 martensitic steel, J. Mater. Process. Technol. 211 (2011) 2085-2090.

[33] F. Di Gabriele, A. Doubkova, A. Hojna, Investigation of the sensitivity to EAC of steel T91 in contact with liquid LBE, J. Nucl. Mater. 376 (2008) 307–311.

[34] X. Gong, P. Marmy, L. Qin, B. Verlinden, M. Wevers, M. Seefeldt, Temperature dependence of liquid metal embrittlement susceptibility of a modified 9Cr-1Mo steel under low cycle fatigue in lead-bismuth eutectic at 160-450 °C, J. Nucl. Mater. 468 (2016) 289-298.

[35] V. Popovich, I. Dmukhovskaya, Rebinder effect in the fracture of Armco iron in liquid metals, Sov. Mater. Sci. 14 (4) (1978) 365–370.

[36] I. Dmukhovskaya, N. Yaremchenko, Y. Zima, V Popovich, Influence of temperature on the character of failure of Armco iron in liquid-metal media, Sov. Mater. Sci. 19 (5) 1984, 431-434.

[37] A. Hojna, F. Di Gabriele, J. Klecka, J. Burda, Behaviour of the steel T91 under uniaxial and multiaxial slow loading in contact with liquid lead, J. Nucl. Mater. 466 (2015) 292-301.

[38] Di Gabriele F., Hojná A., Chocholousek M., Klecka J. Behavior of the steel T91 under multi axial loading in contact with liquid and solid Pb. Metals 7(9) (2017) 342.

[39] A. Hojná, F. Di Gabriele, M. Chocholoušek, L. Rozumová, J. Vít, Effect of applied stress on T91 steel performance in liquid lead at 400 °C, Materials 10(12) (2018) 2512.

[40] V.P. Sobolev, A. Gessi., Chapter 2: Thermophysical and electric properties of liquid lead, bismuth and lead-bismuth eutectic, in Handbook on lead–bismuth eutectic alloy and lead properties, materials compatibility, thermal-hydraulics and technologies, OECD/NEA, 2015, pp 27-142.

[41] L. Martinelli, Chapter 3: Thermodynamic relationships and heavy liquid metal interaction with other coolants, in Handbook on lead–bismuth eutectic alloy and lead properties, materials compatibility, thermal-hydraulics and technologies, OECD/NEA, 2015, pp 143-184.

[42] S. Gossé, S, Thermodynamic Assessment of Solubility and Activity of Iron, Chromium, and Nickel in Lead Bismuth Eutectic, J. Nucl. Mater. 449 (2014) 122-131.

[43] P. Protsenko, A. Terlain, M. Jeymond, N. Eustathopoulos, Wetting of Fe–7.5%Cr steel by molten Pb and Pb–17Li, J. Nucl. Mater. 307 (2002) 1396-1399.

[44] P. Protsenko, N. Eustathopoulos, Surface and grain boundary wetting of Fe based solids by molten Pb and Pb-Bi eutectic, J. Mater. Sci. 40 (2005) 2383-2387.

[45] D. A. Kambolov, A. Z. Kashezhev, R. A. Kutuev, M. Kh. Ponezhev, V. A. Sozaev, A. Kh. Shermetov, Polytherms of density and surface tension of bismuth lead and of angle of wetting of high nickel and ferritic–martensitic steels by the Pb–Bi alloy, High Temperature 52(3) (2014) 381-384.

[46] F. Balbaud-Celerier, P. Deloffre, A. Terlain, A. Rusanov, Corrosion of metallic materials in flowing liquid lead-bismuth, J. Phys IV France 12 (2002) 177-190.

[47] L. Martinelli, T. Dufrenoy, K. Jaakou, A. Rusanov, F. Balbaud-Célérier, High temperature oxidation of Fe–9Cr–1Mo steel in stagnant liquid lead–bismuth at several temperatures and for different lead contents in the liquid alloy, J. Nucl. Mater. 376(3) (2008) 282-288.

[48] C. Lesueur, D. Chatain, C. Bergman, P. Gas, F. Baqué. Analysis of the stability of native oxide films at liquid lead/metal interfaces, J. Phys IV 12, 2002, 155-162.

[49] A.T. Hasouna, K. Nogi, K. Ogino, Influence of Oxygen Partial Pressure on the Wettability of Solid Fe by Liquid Bi, Mater. Trans. JIM, 31(4) (1990) 302-306

[50] L. Martinelli, F. Balbaud-Célérier, A. Terlain, S. Delpech, G. Santarini, J. Favergeon, G. Moulin, M. Tabarant, G. Picard, Oxidation mechanism of a Fe–9Cr–1Mo steel by liquid Pb–Bi eutectic alloy (Part I), Corros. Sci. 50(9) (2008) 2523-2536.

Table 1 : Chemical composition of the T91 steel.

Element	C	Cr	Mo	Nb	V	Si	P	Mn	Ni	Al	N	Fe
wt %	0.102	8.99	0.89	0.06	0.21	0.22	0.021	0.38	0.11	0.0146	0.0442	Bal

Table 2 : SPT results at 300 °C in air, in LBE and in bismuth : the maximum load F_{max}, the displacement at the maximum laod d_f, the energy at the maximum load J_{fmax} (area under the load versus displacement curve until F_{max}) and the normalized energy at the maximum force (fracture energy per thickness unit) $J_{fmaxNorm}$.

Conditions	F_{max} (N)	d_f (mm)	J_{fmax} (J)	$J_{fmaxNorm}$ (J/mm)
Bi, 0.0005 mm/min	1130±42	0.78±0.14	0.66±0.03	1.31±0.06
Bi, 0.005 mm/min	1245	0.95	0.77	1.52
Bi, 0.05 mm/min	1384	0.96	1.17	1.89
Bi, 0.5 mm/min	1428±46	1.29±0.01	1.09±0.06	2.19±0.09
LBE, 0.0005 mm/min	1116±158	0.69±0.03	0.63±0.06	1.24±0.10
LBE, 0.005 mm/min	1458±8	1.05±0.14	1.05±0.14	2.10±0.28
LBE, 0.05 mm/min	1575±112	1.02±0.08	1.09±0.10	2.18±0.16
LBE, 0.5 mm/min	1720±134	1.38±0.17	1.38±0.25	2.87±0.20
Air, 0.5 mm/min	1946±190	1.67±0.06	2.14±0.33	4.14±0.52

Table 3 : SPT results at 400 °C in air, in LBE, in bismuth and in lead : the maximum load F_{max}, the displacement at the maximum laod d_f, the energy at the maximum load J_{fmax} (area under the load versus displacement curve until F_{max}) and the normalized energy at the maximum force (fracture energy per thickness unit) $J_{fmaxNorm}$.

Conditions	F_{max} (N)	d_f (mm)	J_{fmax} (J)	$J_{fmaxNorm}$ (J/mm)
Bi, 0.0005 mm/min	1522	1.35	1.27	2.47
Bi, 0.005 mm/min	1235	0.92	0.78	1.55
Bi, 0.05 mm/min	1418	1.14	0.94	1.89
Bi, 0.5 mm/min	1285	1.22	0.94	1.83

LBE, 0.0005 mm/min	1384	0.95	0.90	1.8
LBE, 0.005 mm/min	1230±17	0.85±0.13	0.74±0.15	1.47±0.33
LBE, 0.05 mm/min	1167±19	0.92±0.01	0.72±0.05	1.46±0.02
LBE, 0.5 mm/min	1282±88	1.21±0.16	0.94±0.16	1.87±0.33
Pb, 0.0005 mm/min	1571	1.38	1.35	2.76
Pb, 0.005 mm/min	1216	1.13	0.71	1.45
Pb, 0.05 mm/min	1220	1.13	0.75	1.13
Pb, 0.5 mm/min	1280	1.42	0.99	1.93
Air, 0.5 mm/min	1707±48	1.64±0.1	1.58±0.12	3.21±0.22

Table 4 : SPT results at 250 °C in air and in LBE : the maximum load F_{max}, the displacement at the maximum laod d_f, the energy at the maximum load J_{fmax} (area under the load versus displacement curve until F_{max}) and the normalized energy at the maximum force (fracture energy per thickness unit) $J_{fmaxNorm}$.

Conditions	F_{max} (N)	d_f (mm)	J_{fmax} (J)	$J_{fmaxNorm}$ (J/mm)
LBE, 0.0005 mm/min	1395	1.12	1.08	2.16
LBE, 0.005 mm/min	1434±200	0.98±0.03	0.98±0.03	1.91±0.02
LBE, 0.05 mm/min	1497±83	1.12±0.11	1.06±0.11	2.14±0.20
LBE, 0.5 mm/min	1696±67	1.78±0.14	1.83±0.02	3.69±0.10
Air, 0.5 mm/min	1796±98	1.64±0.02	1.77±0.02	3.68±0.04

Table 5 : The lead and bismuth activities in LBE at SPT temperatures (calculated according recommended formula in [41]).

	250 °C	300 °C	400 °C
Bismuth	0.426	0.436	0.450
Lead	0.301	0.312	0.328

Table 6 : The surface tension (N/m) of liquid lead, liquid bismuth and liquid LBE at SPT temperatures (calculated according recommended formula in [40]).

	Lead	Bismuth	LBE
250 °C			$406.7\ 10^{-3}$
300 °C		$373.6\ 10^{-3}$	$402.7\ 10^{-3}$
400 °C	$449.9\ 10^{-3}$	$365.5\ 10^{-3}$	$394.7\ 10^{-3}$

Table 7 : The oxygen limit solubility in molten lead, bismuth and LBE in weight % (calculated according recommended formula in [41]).

	Lead	Bismuth	LBE
250 °C			$2.31\ 10^{-6}$
300 °C		$1.6\ 10^{-5}$	$1.13\ 10^{-5}$
400 °C	$5.47\ 10^{-5}$	$1.8\ 10^{-4}$	$1.3\ 10^{-4}$

Fig. 1. Microstructure of the martensitic T91 steel observed by optical microscope.

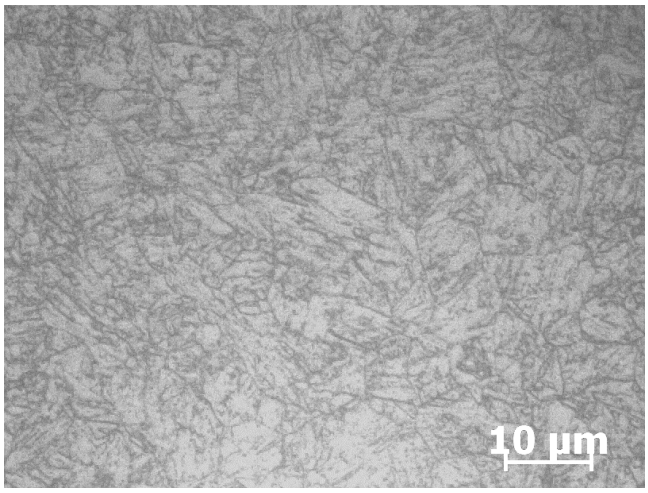


Fig. 2. Small Punch Test device for tests in liquid metal.

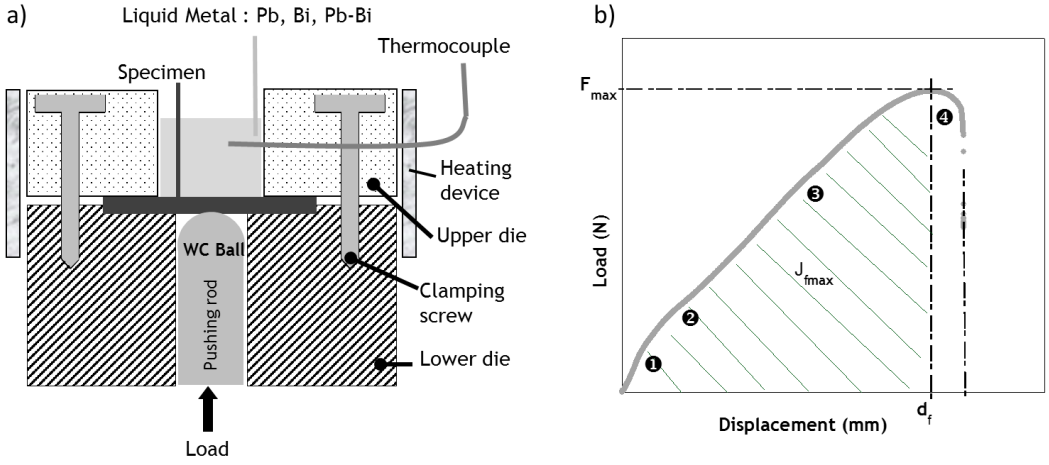


Fig. 3. SPT load-displacement curves of the T91 steel tested in bismuth (a)) and in LBE (b)) saturated in oxygen at 300 °C and at different displacement velocities.

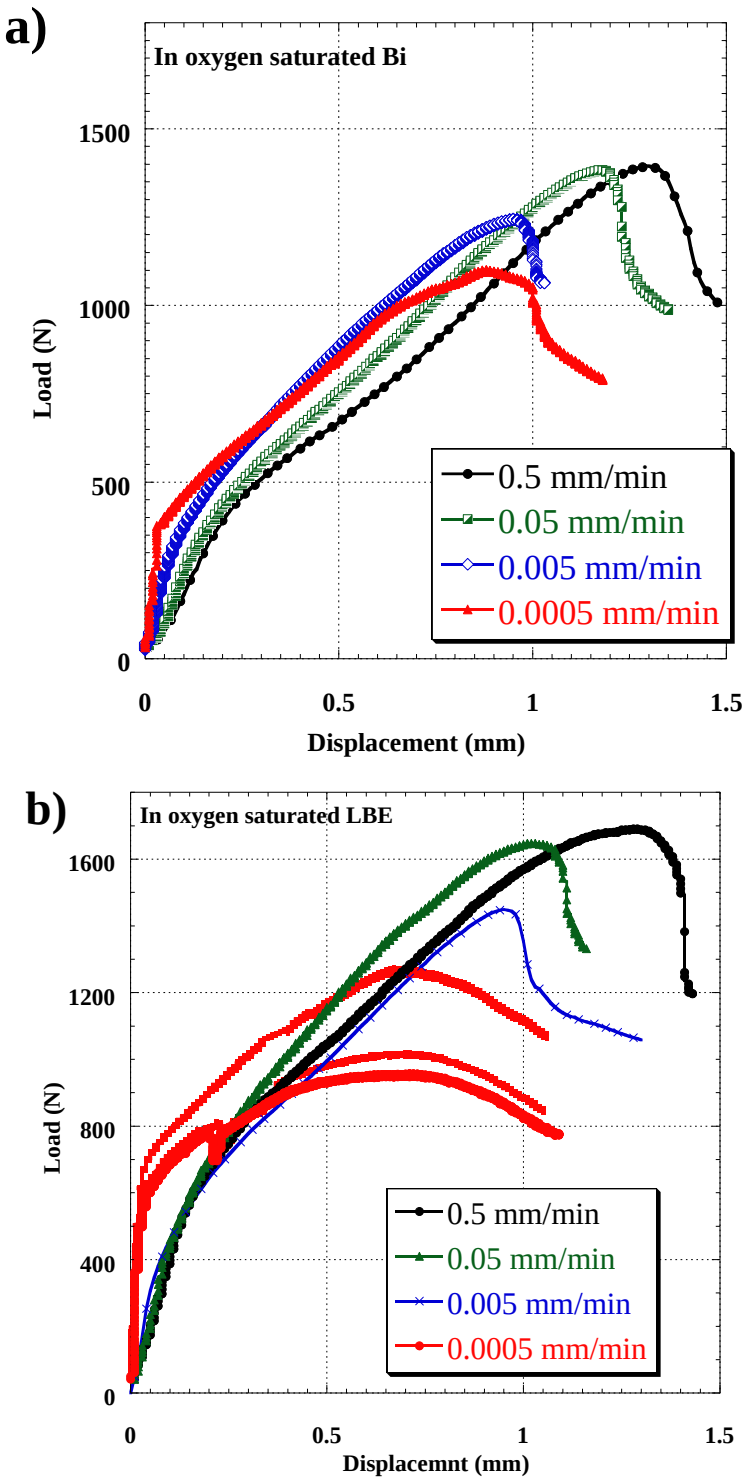


Fig. 4. SEM macro-view of the dome and of the fracture surface of the T91 steel tested in oxygen saturated bismuth at 300 °C, at 0.5, 0.05, 0.005 mm/min.

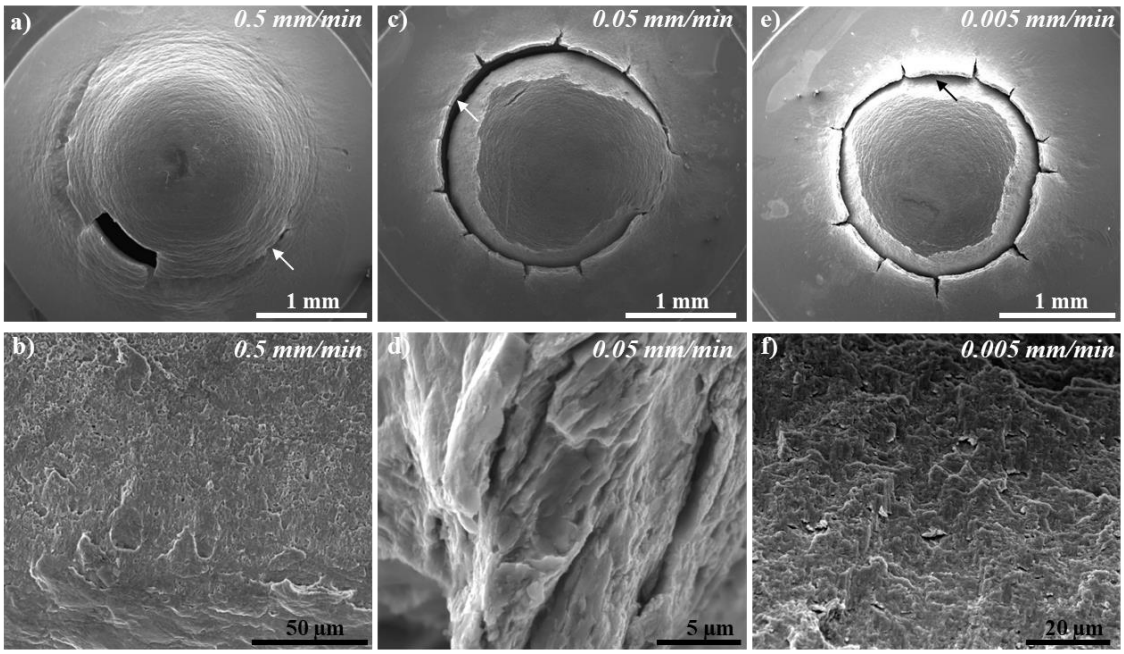


Fig. 5. SEM macro-view of the dome and of the fracture surface of the T91 steel tested in oxygen saturated lead-bismuth eutectic at 300 °C, at 0.5, 0.05, 0.005, 0.0005 mm/min.

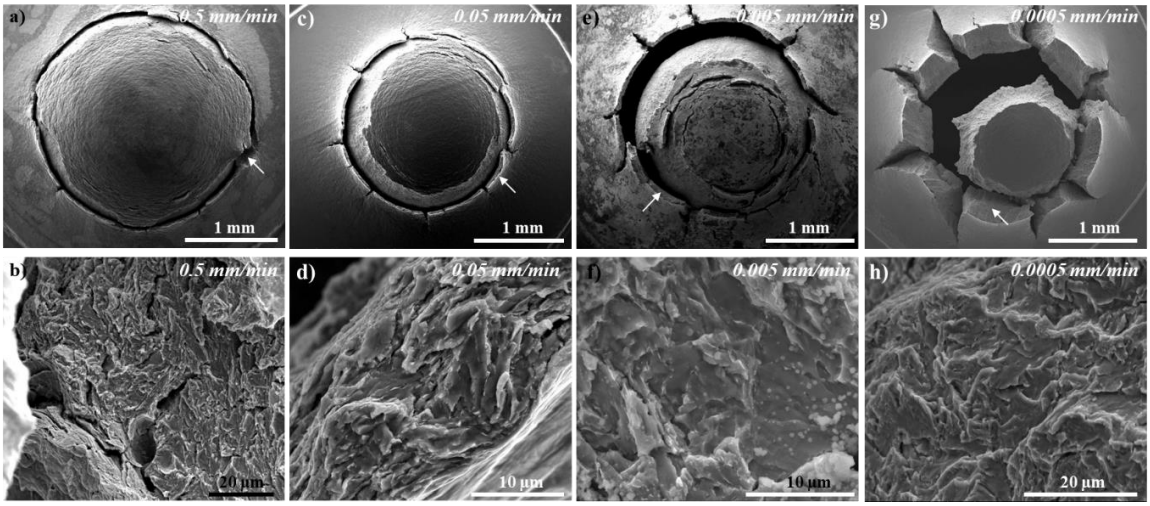
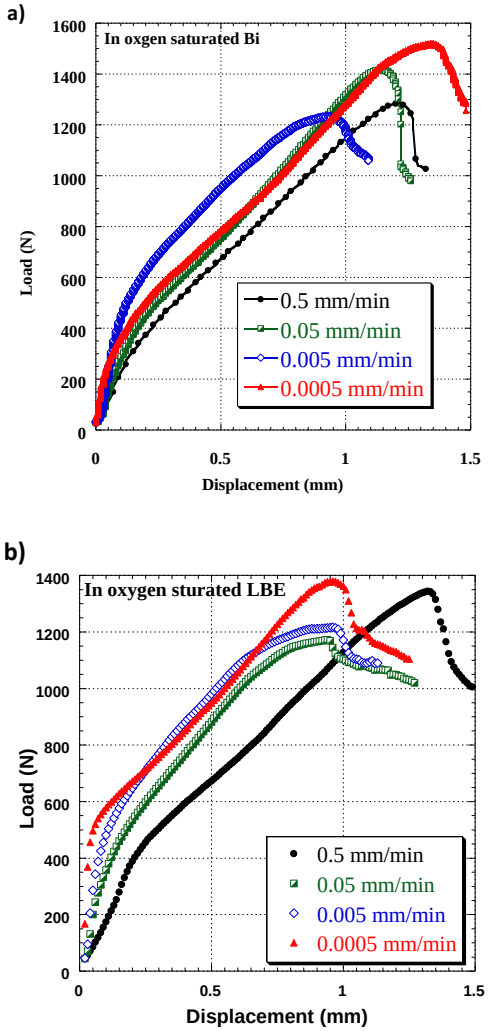


Fig. 6. SPT load-displacement curves of the T91 steel tested in bismuth (a)), in LBE (b)) and in lead (c)) saturated in oxygen at 400 °C and at different displacement velocities.



c)

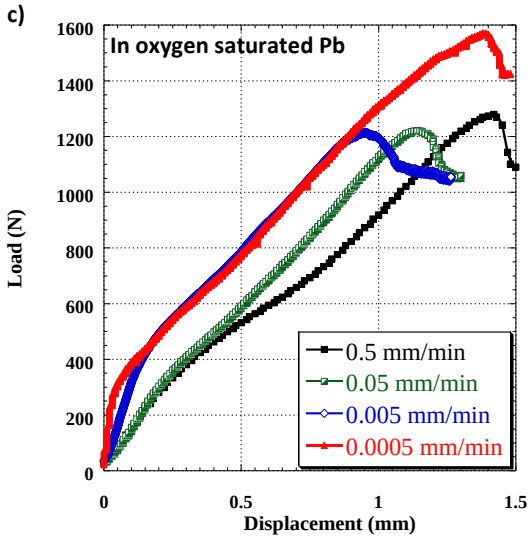

In oxygen saturated Pb
Load (N)
Displacement (mm)
0
200
400
600
800
1000
1200
1400
1600
0
0.5
1
1.5
0.5 mm/min
0.05 mm/min
0.005 mm/min
0.0005 mm/min

Fig. 7. SEM macro-view of the dome and of the fracture surface of the T91 steel tested at 400 °C in oxygen saturated Bi (a), b), c), d), i), j)), in oxygen saturated lead-bismuth eutectic (e), f), k)) and in oxygen saturated Pb (g), h), l)).

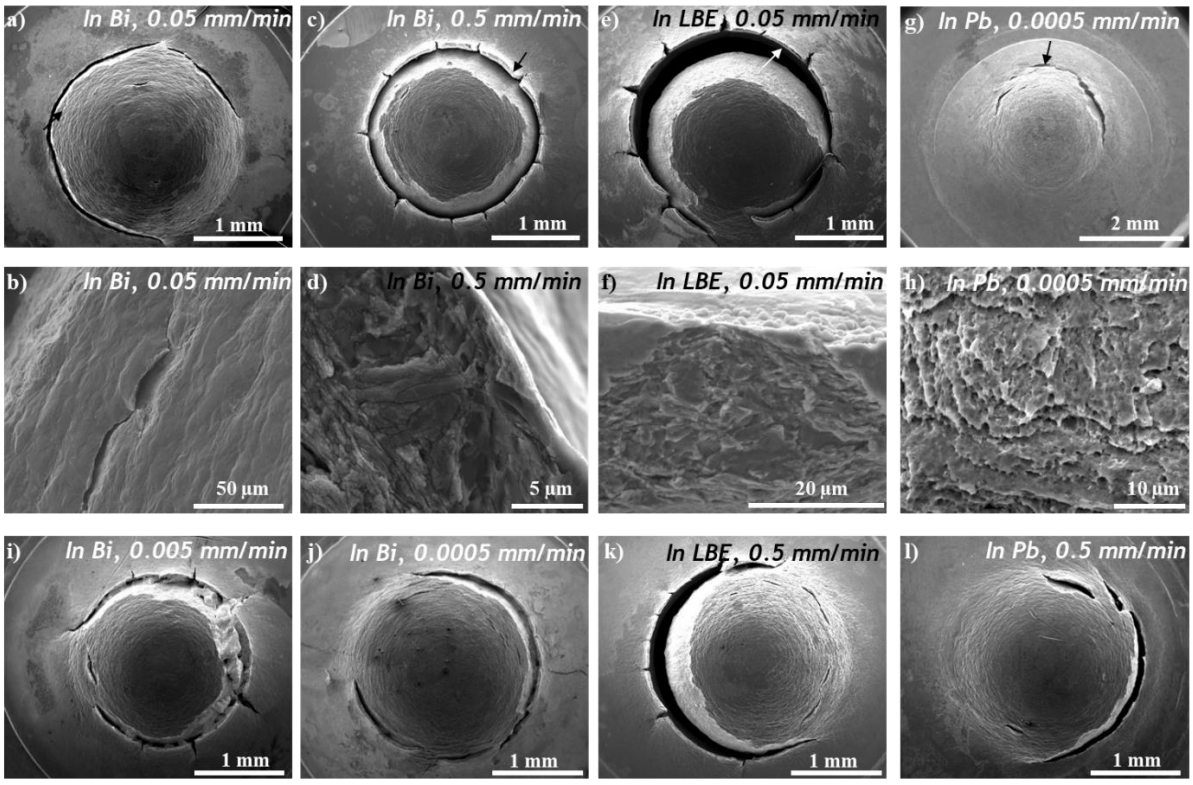


Fig. 8. SPT load-displacement curves of the T91 steel tested in LBE saturated in oxygen at 250 °C and at different displacement velocities.

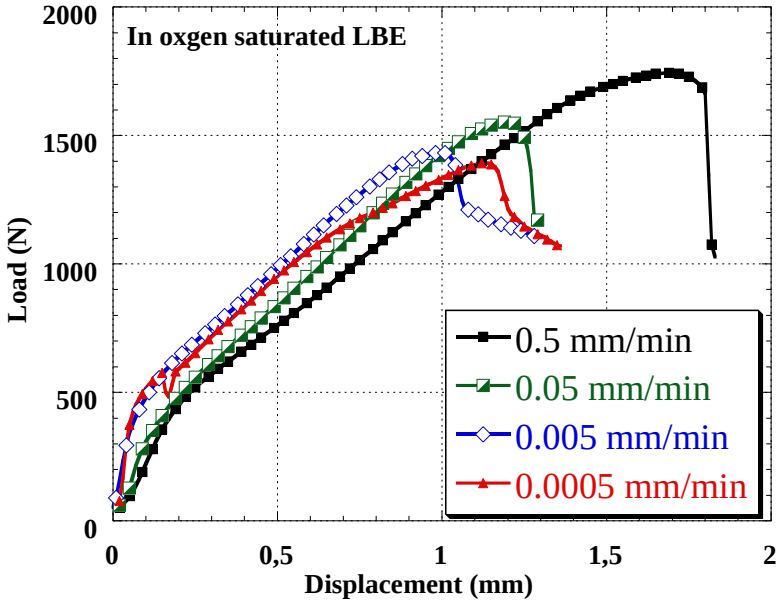


Fig. 9. SEM macro-view of the dome and of the fracture surface of the T91 steel tested in oxygen saturated lead-bismuth eutectic at 250 °C, at 0.5, 0.05, 0.005, 0.0005 mm/min.

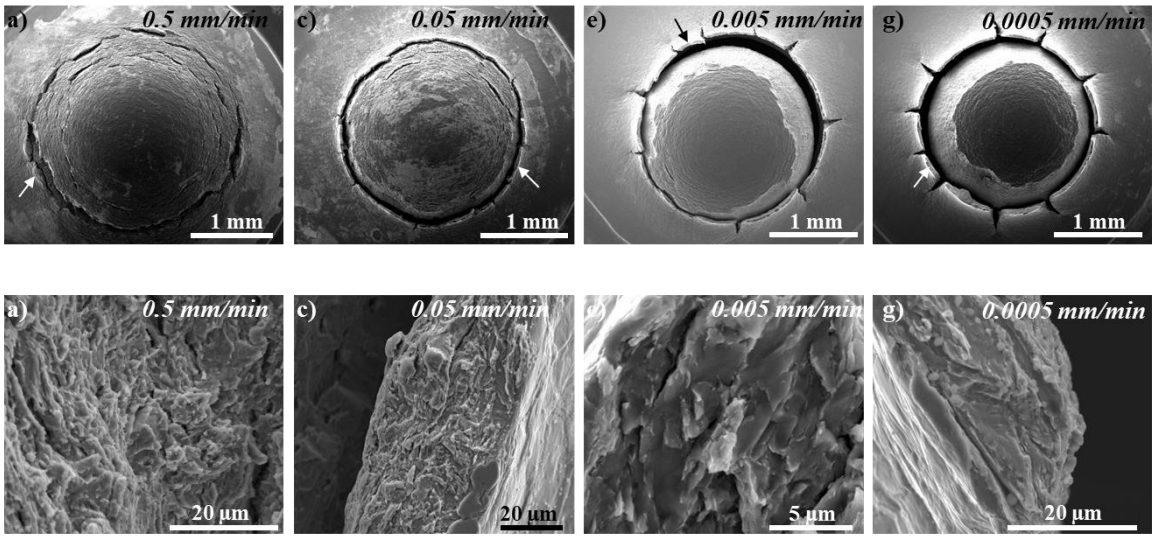


Fig. 10. Evolution of the normalized fracture energy at Fmax versus the crosshead speed and the environment (SPT at 300 °C).

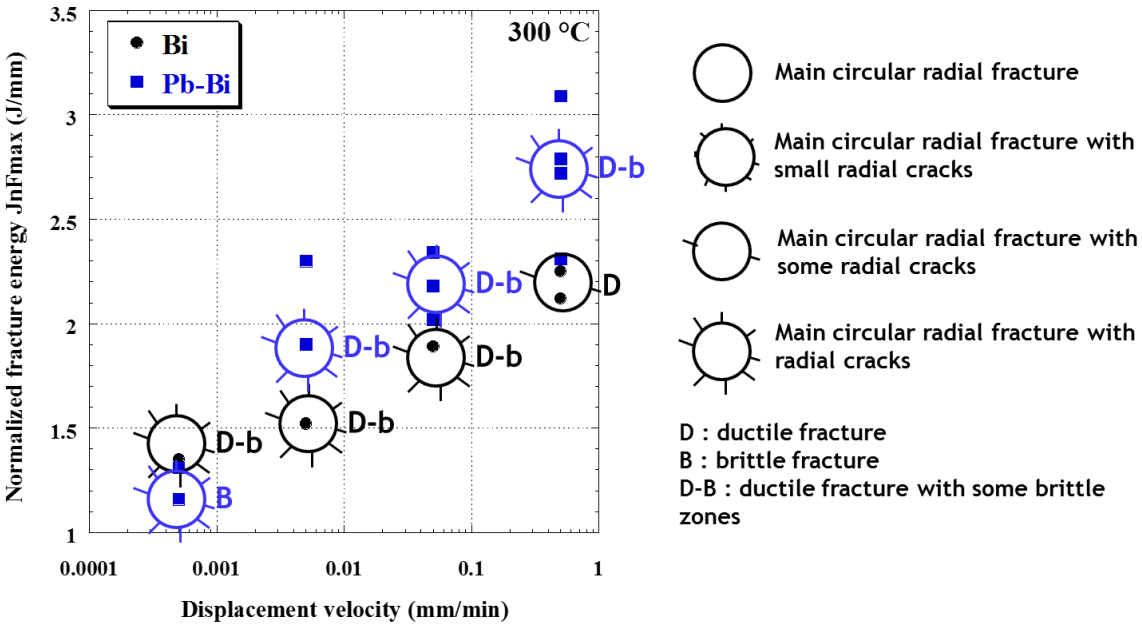


Fig. 11. Evolution of the normalized fracture energy at Fmax versus the crosshead speed and the environment (SPT at 400°C).

